Cobalt–Oxygen Bond Homolysis in the Bench-Stable (Salen*)Cobalt(III) Acetate Complex: Insight into the Organometallic Mediated Radical Polymerization of Diverse Monomers

Maxime Michelas, Sofia Mcgee-renedo, Jirong Wang, Rinaldo Poli, Antoine Debuigne, Christophe Fliedel

Macromolecular Chemistry and Physics

Macromolecular Chemistry and Physics
www.mcp-journal.de

RESEARCH ARTICLE OPEN ACCESS

Cobalt–Oxygen Bond Homolysis in the Bench-Stable (Salen*)Cobalt(III) Acetate Complex: Insight into the Organometallic Mediated Radical Polymerization of Diverse Monomers

Maxime Michelas[1] | Sofia McGee-Renedo[2] | Jirong Wang[1] | Rinaldo Poli[1,3] | Antoine Debuigne[2] | Christophe Fliedel[1]

[1]CNRS, Laboratoire de Chimie de Coordination (LCC), Université de Toulouse (UPS), INPT, Toulouse, Cedex, France | [2]Center for Education and Research on Macromolecules (CERM), CESAM Research Unit, University of Liège, Liège, Belgium | [3]Institut Universitaire de France, Paris, France

Correspondence: Antoine Debuigne (adebuigne@uliege.be) | Christophe Fliedel (christophe.fliedel@lcc-toulouse.fr)

Received: 24 April 2025 | **Revised:** 18 June 2025

Funding: This study was funded by the ANR (Agence Nationale de la Recherche) through the POLYSWITCH project (grant ANR-19-CE07-0031-01) and by the CNRS (Centre National de la Recherche Scientifique).

Keywords: radical polymerization | cobalt | salen-type ligand | catalytic chain transfer | block copolymer

ABSTRACT

Thermal activation of the [(Salen*)Co^{III}(OAc)] (Salen* = (*R*,*R*)-*N*, *N*'-bis(3,5-di-*tert*-butylsalicylidene)-1,2-cyclohexanediamine) complex (**1**) allows to initiate the radical polymerization of methyl methacrylate (MMA) and methyl acrylate (MA) via Co^{III}—O bond homolysis. Catalytic chain-transfer has been identified as the dominant mechanism in the case of MMA, leading predominantly to α-H and ω-unsaturated polymeric chains, as deduced from MALDI-ToF mass spectrometry (MS). In contrast, the organometallic-mediated radical polymerization (OMRP) of MA is well-controlled, and the pseudo-livingness of the process could be highlighted by a linear increase of poly(methyl acrylate) (PMA) molar mass with the conversion, low dispersities, and the successful chain-extension of a Co^{III}-capped PMA macroinitiator with *n*-butyl acrylate (BA), leading to a well-defined poly(methyl acrylate)-block-poly(*n*-butyl acrylate) (PMA-*b*-PBA) block copolymer. MALDI-ToF MS and multinuclear NMR analyses allowed to identify two competing initiation processes for the OMRP of MA.

1 | Introduction

Reversible-deactivation radical polymerization (RDRP) has become a major tool for the preparation of well-defined polymeric materials of diverse architectures [1, 2]. Radical polymerization can be performed in solution, bulk monomer, dispersed media [3], or on a solid surface [4, 5]. The high tolerance of radical polymerization towards functional groups and the chain-end(s) control allow the production of valuable functional materials for applications in various fields, including electronics, coatings, or biomedicine [6–8]. Reversible addition-fragmentation chain-transfer (RAFT) polymerization and atom-transfer radical polymerization (ATRP) are currently dominating the field of RDRP. While the former makes use of organic molecules, such as trithiocarbonates, xanthates, and dithiocarbamates (general formula of the type [Z—C(=S)S—R^3], Z = SR [1], OR [1], NR^{1}R^2, respectively, R^n = any organic group) as chain-transfer agents to control the polymerization by the degenerate transfer (DT) principle [9], the latter is based on the ability of a redox-active transition metal (typically copper or iron) complex ([L/Mt^x], L = ligand, Mt = transition metal, x = oxidation state) to reversibly abstract a halogen atom (Y)

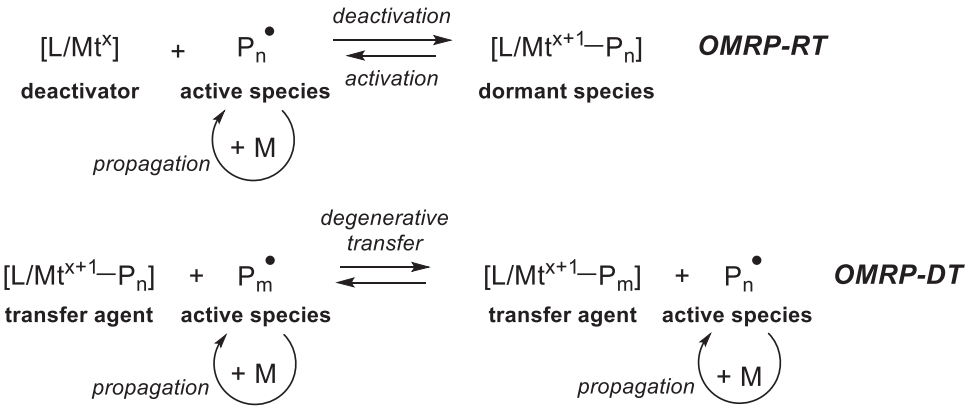

SCHEME 1 | OMRP-RT and OMRP-DT equilibria.

from a polymeric dormant chain (P_n-Y) to create an active radical/propagating chain ($P_n^{\bullet}$) and the moderating complex [L/Mt^{x+1}-Y] for control of the chain growth by the reversible termination (RT) principle [10–12]. Organometallic-mediated radical polymerization (OMRP) is another RDRP method that takes advantage of the use of metal complexes to reversibly deactivate the active chains [13, 14]. In the reversible termination mode (OMRP-RT), the deactivation consists of the trapping of the propagating/active radical species ($P_n^{\bullet}$) by the complex in its lower oxidation state ([L/Mt^{x}], deactivator), leading to the corresponding organometallic complex in its higher oxidation state ([L/Mt^{x+1}-P_n], dormant species), via a metal–carbon bond formation and the activation occurs by the reverse process, namely homolytic cleavage of the metal–carbon bond in the dormant species to regenerate the propagating radical species ($P_n^{\bullet}$) and the deactivator ([L/Mt^{x}]) (Scheme 1, top) [15, 16]. Using an excess radical initiator, OMRP can also work under degenerative transfer mode (OMRP-DT) (Scheme 1, bottom). Although OMRP may suffer, as any other RDRP techniques, from limitations and side reactions [17, 18], it has achieved several breakthroughs in the controlled polymerization of less-activated monomers (LAMs), such as vinyl acetate (VAc) [19, 20], vinyl amides [21, 22], vinylidene fluoride (VDF) [23] and so forth, which remained challenging for other RDRP methods [24, 25]. Cobalt complexes are clearly dominating the area of OMRP [26–28], albeit a few other transition metal complexes have also given interesting results [29–33]. Among the various cobalt complexes evaluated in OMRP, those supported by porphyrins and Schiff bases are quite efficient for the controlled polymerization of more activated monomers (MAMs) such as acrylates [34, 35], while [Co(acac)$_2$] (acac = acetylacetonate) and other bis(β-diketonate) analogs proved to be excellent moderators for the controlled polymerization of LAMs [20, 23, 36, 37].

OMRP-RT initiation can be realized either in a reverse mode, using an appropriate primary radical source, such as AIBN (2,2′-azobis(2-methylpropionitrile)), and the [L/Mt^{x}] deactivator (Scheme 2a), or in a direct mode using an appropriate [L/Mt^{x+1}-R_0] unimolecular initiator (Scheme 2b, c). Both approaches were successfully applied for the preparation of various well-defined polymeric materials [20, 26, 38]. As a specific case of reverse mode OMRP initiation, redox-initiated OMRP systems combining peroxides with [Co(acac)$_2$], either alone or in the presence of reducing agents such as ascorbic or citric acid, have been investigated. When used alone, peroxides such as benzoyl peroxide or lauroyl peroxide can interfere with the OMRP process through redox reactions with the cobalt complex, compromising its role as a mediating species. However, combining the peroxide with a reductant enhances the polymerization rate while preserving the control character of the cobalt-mediated radical polymerization [39]. Nevertheless, direct initiation appears much more attractive, because i) it does not require the use of thermally sensitive azo- or peroxo-initiators and air-sensitive/easily oxidized [L/Mt^{x}] moderators and ii) it allows the introduction of the corresponding "R_0" group from the [L/Mt^{x+1}-R_0] unimolecular initiator at the chain end, which may be of interest for further applications or modifications (Scheme 2b, c) [40]. However, most of the [L/Mt^{x+1}-R_0] initiators reported until now are thermally- and/or air-sensitive compounds and the diversity of R_0 groups remains limited (Scheme 2b). Therefore, the development of bench-stable and efficient unimolecular initiators via a synthetic approach that allows the introduction of various R_0 groups remains of particular interest (Scheme 2c) [40]. Due to their large diversity and availability, carboxylic acid derivatives appeared to us as the building blocks of choice for the development of such stable and "functional" unimolecular OMRP initiators, provided that suitable conditions can be found to generate carboxylate radicals and that these are able to initiate an OMRP process. With this aim, we recently reported the synthesis of the air-stable [Co^{III}(acac)$_2$(O$_2$CPh)] complex, by simple reaction between [Co^{II}(acac)$_2$] and commercially available benzoyl peroxide (2:1 ratio), and showed that it is able to readily initiate the OMRP of VAc [41]. The carboxylate moiety appeared to bring together the appropriate levels of stability and reactivity for the desired application. However, this strategy still suffered from the need to synthesize other peroxide reagents, (RCOO)$_2$ for $R \neq Ph$, to tailor the polymer α-chain-end. Therefore, we considered the possibility to access other unimolecular cobalt(III) carboxylate initiators of the type [L/Co^{III}(O$_2$CR$_0$)], directly from the corresponding (pro)ligand, cobalt precursor, and carboxylic acid, and to study their ability to initiate and control an OMRP process.

To our purpose, we turned our attention towards cobalt complexes of Salen-type ligands (unsubstituted Salen = *N*, *N*'-ethylenebis(salicylideneiminato), Figure 1, left) for the following reasons. On one hand, a few studies mentioned the use of cobalt complexes of Salen-type ligands as moderators and/or

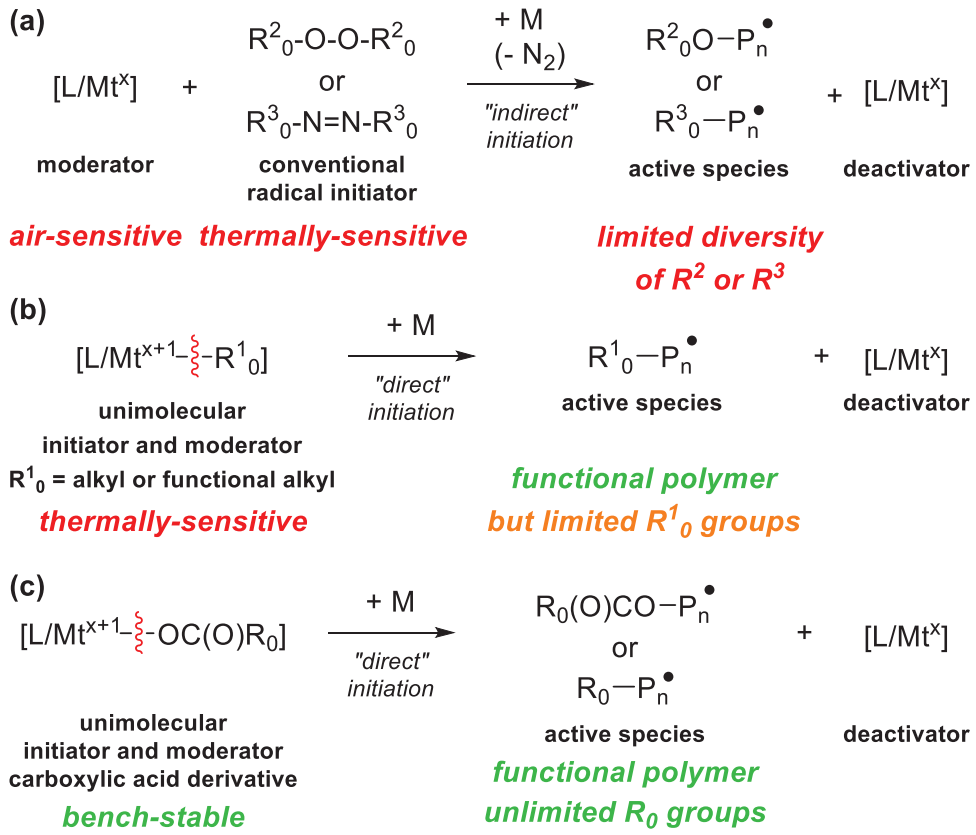

SCHEME 2 | OMRP direct initiation (a), indirect initiation with an organometallic initiator (b), and indirect initiation with a metal carboxylate initiator (c).

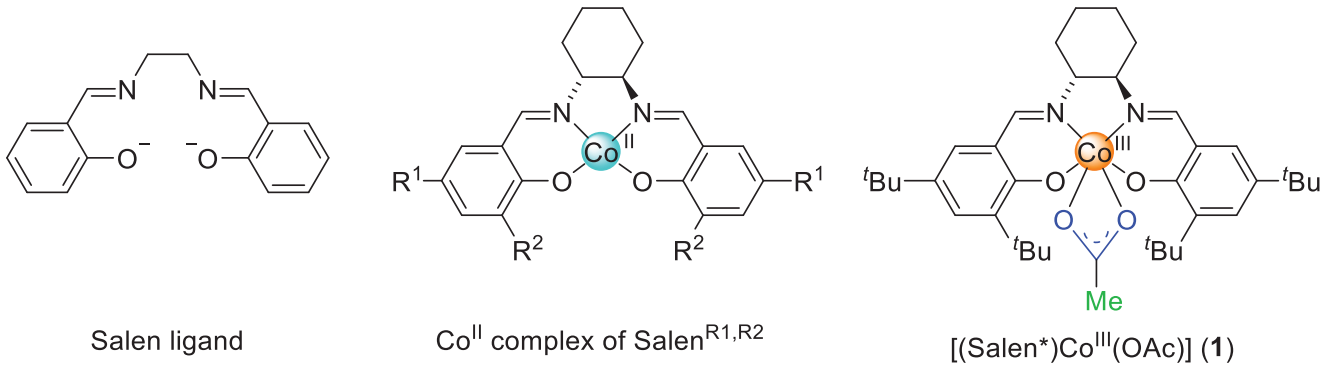

FIGURE 1 | Structures of the Salen ligand, cobalt(II) complexes of Salen-type ligands, and the [(Salen*)Co^{III}(OAc)] (**1**) complex.

(co)initiators in radical polymerization but none of them involved a bench-stable initiator with a Co—O bond. Storr, Shaver, and coworkers applied cobalt(II) complexes of sterically and electronically tuned Salen-type ligands (*ortho*- and *para*-substituents on the phenol moieties, see Figure 1, middle) to the OMRP of styrene (St), methyl methacrylate (MMA), and VAc, in the reversible termination mode (0.6 equiv. AIBN or V-70 vs. Co), and a controlled polymerization of VAc could be achieved with the *o*-^{t}Bu-*p*-OMe-decorated Salen complex [42]. The group of Peng showed that the cobalt(II) complex [(Salen*)Co^{II}] (Salen* = (*R*, *R*)-*N*, *N*'-bis(3,5-di-*tert*-butylsalicylidene)-1,2-cyclohexanediamine, see Figure 1, middle) readily mediates the controlled radical polymerization of methyl acrylate (MA) and VAc, in the DT mode, using excess AIBN (6.5 or 10 equiv. vs. Co) in benzene at 60°C [34]. More recently, Wang, Poli and coworkers showed that [(Salen*)Co^{II}] could be used as moderator to produce poly(vinyl acetate)-*b*-polycarbonates via sequential ORMP-DT of VAc and ROcoP of CO_2/epoxides [43] and polyester-*b*-polyacrylates via sequential ROcoP of anhydrides/epoxides and light-initiated OMRP of acrylates [44]. These block copolymers were obtained through original and unprecedented switches of the polymerization mechanisms. Finally, Peng, Fu and coworkers demonstrated that a combination of the cobalt(III) complex [(Salen*)$Co^{III}(CO_2Me)$] and the 2,4,6-trimethylbenzoyl diphenylphosphine oxide (TPO) photoinitiator (1:1 ratio) also allows a fast and controlled polymerization of acrylates, acrylamides and vinyl acetate through

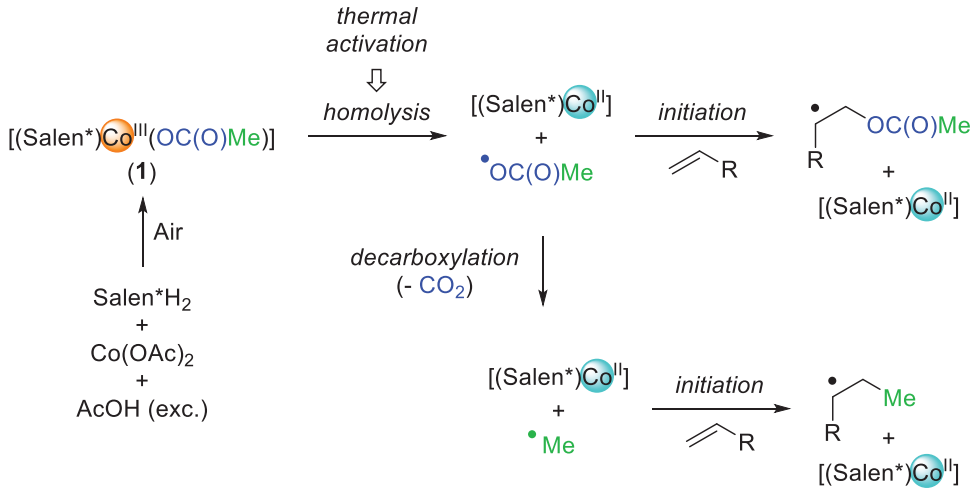

SCHEME 3 | Possible radical polymerization initiation paths by [(Salen*)Co(OAc)] (**1**), with (bottom) and without (top) decarboxylation.

light-initiated OMRP [45]. On the other hand, Jacobsen and coworkers observed that a cobalt(II) complex of a Salen-type ligand can be readily and cleanly oxidized in air, in the presence of benzoic acid or acetic acid, to the corresponding Salen*-cobalt(III) benzoate or acetate complexes [46–48]. Furthermore, the [(Salen*)Co^{III}(OAc)] complex (Figure 1, right) could also be obtained in good yields (92%) by reaction between the free pro-ligand, anhydrous [$Co(OAc)_2$] and excess glacial AcOH in the air (presumably serving as an oxidant) [49]. It was then successfully applied to a landmark hydrolytic kinetic resolution (HKR) of terminal epoxides and has later found several other applications, such as epoxides and epoxides/CO_2 (co)polymerization [50–52], but has not been applied to radical polymerization, to the best of our knowledge. The present work explores for the first time the potential of [(Salen*)Co^{III}(OAc)] to act as an initiator for the OMRP of various vinyl monomers, including conjugated and non-conjugated ones.

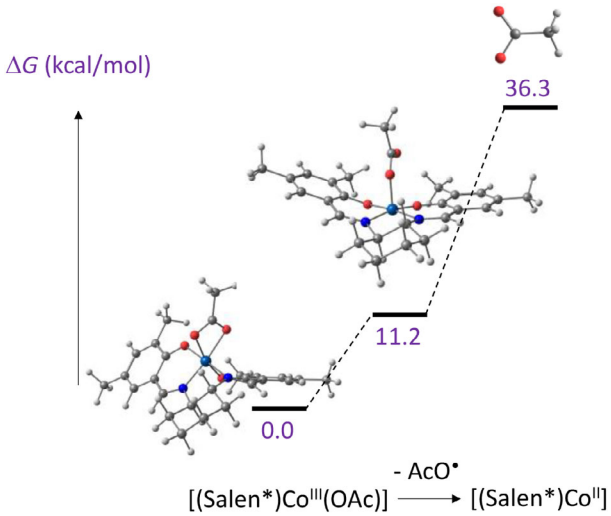

FIGURE 2 | Gibbs energy profiles for the dissociation of the AcO• radical from the [(Salen*)Co(OAc)] complex **1**.

2 | Results and Discussion

2.1 | Complex Stability/Reactivity and DFT Calculations

The H_2Salen* pro-ligand [53] and the corresponding cobalt(III) acetate complex [(Salen*)Co^{III}(OAc)] (**1**) [54] were prepared according to published procedures (Scheme 3). The ability of complex **1** to generate primary acetate radicals (•OAc) and therefore act as an unimolecular initiator of radical polymerization, under thermal activation, was then evaluated both computationally and experimentally with various vinyl monomers (see below). The initiation step would imply homolytic cleavage of the Co^{III}—$O_{(OAc)}$ bond, furnishing both the [(Salen*)Co^{II}] complex and a •OAc radical, and the latter may; 1) add to a vinyl monomer and initiate the polymerization or 2) undergo a decarboxylation reaction (—CO_2), leading to the •CH_3 radical, which would then add to the monomer and initiate the polymerization (see Scheme 3 for these two paths). This strategy has previously been seldom explored. In 1982, Kalpagam and coworkers reported that [(Salen)Co^{III}(acac)] thermally affords an acac• radical, able to initiate the radical polymerization of methyl methacrylate, but the characteristics of the resulting polymer were as expected for a free-radical mechanism [55]. More recently, we reported a series of acetato-cobalt(III) [56] and acetylacetonato-cobalt(III) and iron(III) complexes [57] supported by diamino-bisphenolate ligands, however, none of them could thermally initiate a radical polymerization process.

The propensity of complex **1** to generate an AcO• radical by homolytic Co—$O_{(OAc)}$ bond cleavage was studied by DFT calculations. As shown by the Gibbs energy profile depicted in Figure 2, the release of the acetate radical follows a two-step mechanism. First, the acetate switches from a bidentate chelating to a monodentate coordination mode and second, Co—$O_{(OAc)}$ bond homolysis occurs. The overall Gibbs energy for the AcO• dissociation is 36.3 kcal/mol under standard conditions (25°C), of which 11.2 are needed for the initial rearrangement from κ^2 to κ^1 and 25.1 for the homolytic cleavage from the 5-coordinate intermediate complex. The feasibility of the Co—$O_{(OAc)}$ bond homolytic cleavage was further assessed by an NMR experiment consisting in the thermal treatment (12 h at 70°C) of a $CDCl_3$ solution of **1**: the resonances of **1** broadened and new resonances

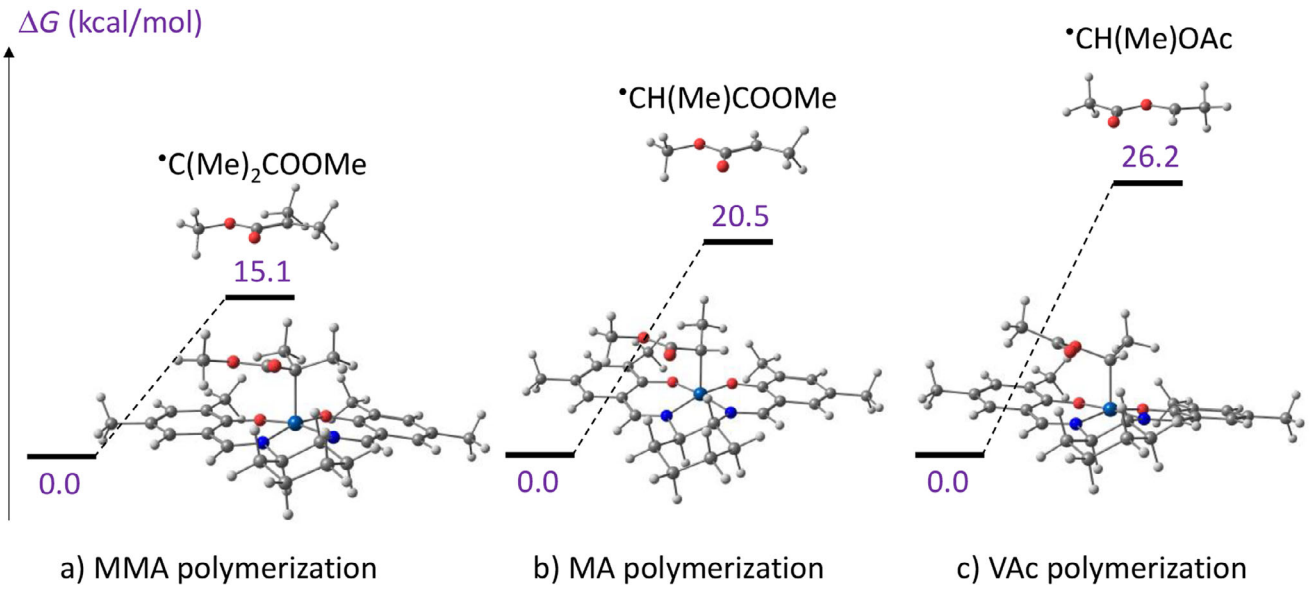

FIGURE 3 | Gibbs energy profiles for the activation of unimer models of the organometallic dormant species formed during the radical polymerization of (a) MMA, (b) MA, and (c) VAc.

attributable to paramagnetic [(Salen*)Co^{II}] appeared (see Figure S1). It should be noticed that, in the presence of Lewis bases such as coordinating solvents or monomers, complex **1** readily forms six-coordinated octahedral neutral adducts of the type [(Salen*)Co(OAc)(L)] (L = Lewis base) [58], which consequently induces the κ^2 to κ^1 coordination mode of the OAc ligand. Indeed, Jacobsen and coworkers always reported L adducts of such [(Salen*)Co(OAc)(L)] complexes (X = OAc, OBz, OTs…; L = H_2O, MeOH, $PhCO_2H$) [47, 49]. Therefore, coordination of a Lewis base may reduce the energetic barrier for the dissociation of the initiating radical. This hypothesis seems supported by our NMR investigations of solutions of complex **1** in the presence of MA or VAc (1:1 complex/monomer ratio). Already at room temperature, the formation of the cobalt(II) species was evident and the spectra further evolved upon gentle warming from 40°C to 70°C (see Figures S2 and S3).

Based on the hypothesis that the generated AcO$^\bullet$ radical is able to initiate the polymerization of MA, MMA and VAc, the resulting PMA$^\bullet$, PMMA$^\bullet$ and PVAc$^\bullet$ growing chain may be reversibly trapped by the [(Salen*)Co^{II}] complex to yield the [(Salen*)Co^{III}-PMA], [(Salen*)Co^{III}-PMMA] and [(Salen*)Co^{III}-PVAc] dormant chains, respectively. The trapping equilibria were estimated using model complexes with the corresponding unimers, namely [(Salen*)Co^{III}-MA-H], [(Salen*)Co^{III}-MMA-H] and [(Salen*)Co^{III}-VAc-H], respectively (see energy profiles in Figure 3). The Gibbs energy gains are in a suitable range to ensure reversible radical trapping. In light of these encouraging results, the ability of complex **1** to initiate and moderate a radical polymerization process was then evaluated.

2.2 | Attempts to Initiate the Radical Polymerization of VAc

As stated in the Introduction, cobalt-based complexes are especially attractive for the controlled polymerization of LAMs under OMRP conditions. Therefore, we initially attempted to use **1** to initiate the radical polymerization of VAc. Unfortunately, heating a reaction mixture composed of complex **1** and VAc, in a 1:200 ratio, up to 90°C for 24 h did not lead to the formation of any polymer (Table S1, entry 1). This observation could be rationalized by either a lack of production of primary radicals ($^\bullet$OAc or $^\bullet$Me) or the irreversible trapping of the generated VAc oligomer. The first hypothesis appears inconsistent with the above-discussed NMR evidence of [(Salen*)Co^{II}] formation from **1**/VAc solutions in C_6D_6 under mild conditions (Figure 3). Thus, the latter hypothesis seems more likely, since the calculated BDEs of the Co^{III}-X bonds in [(Salen*)Co^{III}(κ^1-OAc)(L)] and [(Salen*)Co^{III}(PVAc)] are respectively $\Delta G^{\text{Co-OAc}}$ = 25.1 kcal/mol and $\Delta G^{\text{Co-VAc}}$ = 26.2 kcal/mol. In principle, the [(Salen*)Co^{III}(PVAc)] dormant species may be stabilized even further by chelation of the acetate carbonyl group in the Co-bonded VAc monomer, as shown in previous work for the [$(acac)_2Co^{III}$(PVAc)] dormant species [19, 59, 60]. However, a DFT study of this chelation process on the unimer model indicates that, contrary to the bis(acac) system, this process is endoergic for the (Salen*) system, probably because of additional strain imposed by the needed rearrangement of the Salen* ligand from planar to butterfly (see Figure S4). Incidentally, chelation is even less favored for the unimer models of the PMA and PMMA dormant species, which contain more strained 4-membered rings. The potential of complex **1** to initiate a radical polymerization was therefore evaluated towards more activated monomers, i.e., methyl methacrylate (MMA) and methyl acrylate (MA), and the results are discussed in the following sections.

2.3 | Methyl Methacrylate Polymerization

As shown in Figure 4, complex **1** readily initiated the polymerization of MMA under bulk conditions ([Co]/[MMA] = 1/200) at 60°C without any induction period, reaching nearly 70% conversion after 6 h of reaction (Table S1, entries 2–4). The MMA

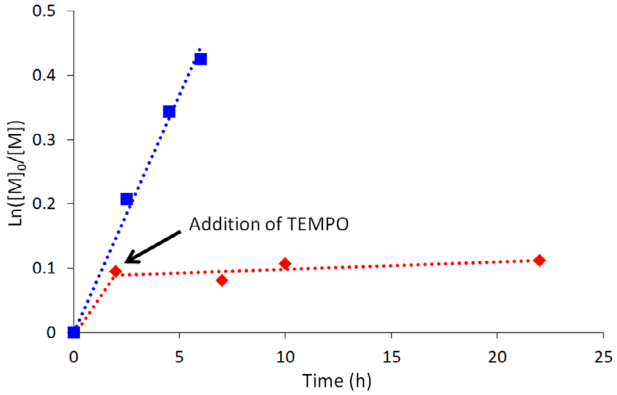

FIGURE 4 | Time dependence of $\ln([M]_0/[M])$ for the bulk polymerization of MMA at 60°C initiated by complex **1** (initial ratio: [**1**]/[MMA] = 1/200) (blue squares) and for the same reaction with addition of excess TEMPO after 2 h (red diamonds). $[M]_0$ and $[M]$ are the MMA concentrations at times 0 and t, respectively.

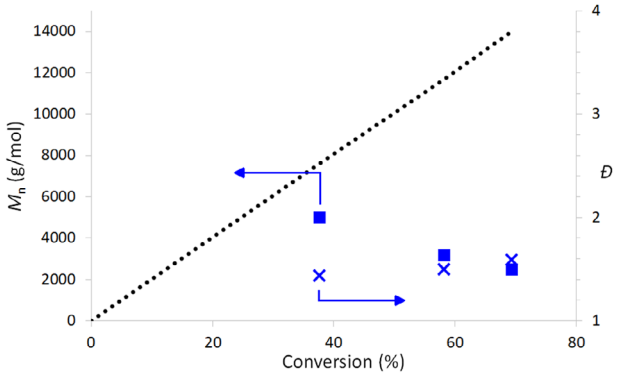

FIGURE 5 | Dependence of PMMA molar masses (M_n, blue squares) and dispersity indexes ($Đ$, blue crosses) on monomer conversion for the bulk polymerization of MMA at 60°C initiated by complex **1** (initial ratio: [**1**]/[MMA] = 1/200). The dotted black line represents the theoretical M_n values.

polymerization rate is first-order in monomer, as assessed by the linear dependence of $\ln([M]_0/[M])$ versus time. The radical character of the polymerization reaction could be assessed by a parallel experiment, in which the radical trap TEMPO was added after 2 h. The MMA conversion stopped (Figure 4), and the recovered polymer samples at longer reaction times exhibited similar characteristics (M_n and $Đ$, Table S1, entries 5–8). Altogether, the aforementioned data highlight that complex **1** is an unimolecular initiator of radical polymerization via homolytic cleavage of the Co^{III}—$O_{(OAc)}$ bond. This is only the second example of a bench-stable OMRP initiator, the first one being $[Co^{III}(acac)_2(OC(O)Ph)]$, recently reported by us for the OMRP of VAc [41].

The GPC analysis of the recovered PMMA samples revealed significantly lower $M_{n,exp}$ than expected for a pseudo-living chain growth ($M_{n,th}$), which decreases with the conversion, and nearly constant and relatively narrow (1.44–1.59) dispersities (Figure 5, Table S1, entries 2–4). These observations suggest the occurrence of catalytic chain transfer (CCT) as an interfering/competing process with OMRP [18, 61]. To support this hypothesis, further

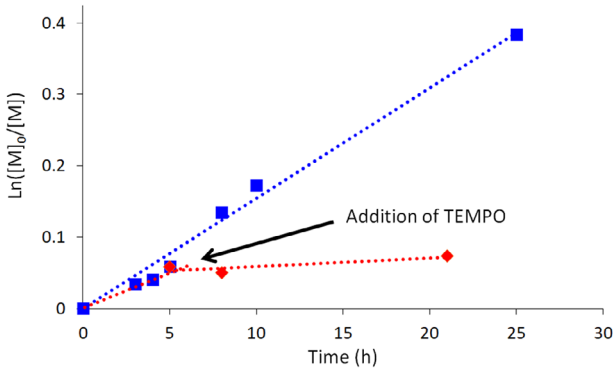

FIGURE 6 | Time dependence of $\ln([M]_0/[M])$ for the bulk polymerization of MA at 70°C initiated by complex **1** (initial ratio: [**1**]/[MA] = 1/200) (blue squares) and for the same reaction with addition of excess TEMPO after 5 h (red diamonds). $[M]_0$ and $[M]$ are the MA concentrations at times 0 and t, respectively.

analyses of the isolated PMMA samples by MALDI-ToF MS were performed (Figures S5 and S6). The latter revealed the presence of a major population of PMMA chains with H as α- and an unsaturated MMA unit as ω-chain ends, both resulting from the CCT process (see Figures S7). Polymerization reactions were performed both at 40°C and 70°C to study the influence of temperature on the level of CCT (vs. OMRP). While the temperature strongly affected the rate of polymerization, much faster at 70°C (74% conv. in 4 h) and much slower at 40°C (66% conv. in 48 h), than at 60°C, in both cases the discrepancy between theoretical and experimental M_n values agrees with extensive CCT during the polymerization process (Table S1, entries 9–11).

While the most active cobalt-based CCT catalysts are supported by tetradentate N_4 ligands, especially cobaloximes and porphyrin derivatives, or by two bidentate N_2 ligands, some precedents with Schiff base ligands were also reported, although their CCT activity remained modest [62, 63]. It might be useful to underline that, although CCT is an unwanted side reaction for our objectives, it is useful for other applications [63].

2.4 | Methyl Acrylate Polymerization

The bulk polymerization of MA, using complex **1** as the initiator, was initially attempted at 60°C. Contrary to MMA, which polymerized rapidly as shown in the previous section, no monomer conversion was observed (Table S2, entry 1). Increasing the polymerization temperature to 70°C, led to a rather slow, but steady polymerization that reached 64% MA conversion after 25 h (Figure 6, Table S2, entry 2–7). The TEMPO quenching experiment highlighted once again the radical nature of the reaction because the conversion stopped after the addition of the radical trap (Figure 6, Table S2, entry 8–10).

As shown in Figure 7, the $M_{n,exp}$ of the recovered PMA samples increased nearly linearly as a function of the conversion, and their dispersities remained relatively narrow (≤1.31, Figure 7, Table S2, entry 2–7). However, the experimental molar masses were much higher than the theoretical ones (black dotted line in Figure 7), reflecting a low initiator efficiency factor (≤0.3). Thus, less than

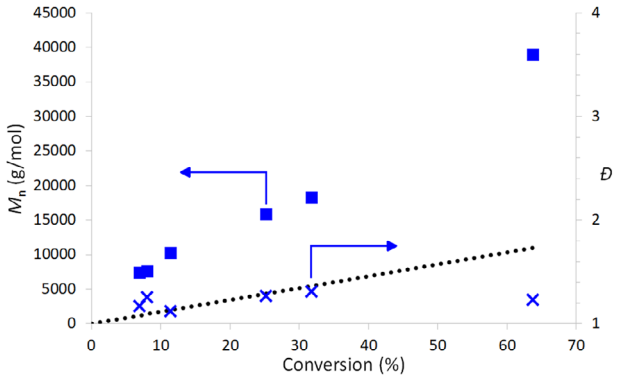

FIGURE 7 | Dependence of PMA molar masses (M_n, blue squares) and dispersity indexes ($Đ$, blue crosses) on monomer conversion for the bulk polymerization of MA at 70°C initiated by complex **1** (initial ratio: [**1**]/[MA] = 1/200). The dotted black line represents the theoretical M_n values.

30% of complex **1** underwent the homolytic cleavage required to start the macromolecular chain growth.

The DFT predictions described above qualitatively agree with these experimental results. As a reminder, the computed Gibbs energy change (ΔG) for the Co^{III}-X homolytic bond cleavage is 20.5 kcal/mol for X = carbomethoxyethyl (PMA model) and 15.1 kcal/mol for X = carbomethoxyisopropyl (PMMA model). Thus, [(Salen*)Co^{II}] has a stronger aptitude to trap the PMA radicals and control the chain growth, whereas the weaker bond with the PMMA radical opens the way to a greater impact of CCT. Note also that the ΔG associated with the Co^{III}—OAc bond cleavage in the initiator (Figure 2) is higher, predicting a slow initiation and thus a low initiator efficiency. However, the fact that no detectable MA polymerization occurred at 60°C, a temperature at which a fast MMA polymerization could be observed, is probably due to a too-slow reactivation of the [(Salen*)Co^{III}CH(COOMe)CH_2OAc] dormant species resulting from the first MA insertion.

In order to confirm the controlled character of the MA polymerization initiated by complex **1** and the possibility to adjust the molar mass of PMA, the MA polymerization was performed again at 70°C using the lower MA/1 ratio of 100 (Table S2, entries 11–15). Again, M_n regularly increased with the monomer conversion (Figure S8), and the SEC chromatograms of the recovered polymers (Figure S9) clearly shifted towards lower elution volume along the monomer conversion, in line with controlled chain growth. The experimental molar masses were again greater than the theoretical ones, and the initiator efficiency factor remained lower than 30% (Table S2, Figure S8). This further confirms the controlled character of the MA polymerization and the possibility to tune the molar mass of the PMA by varying the monomer/complex ratio.

Furthermore, with the objective of improving the initiator efficiency factor, the polymerization of MA was performed at 80°C instead of 70°C (Table S2, entries 16–21). While the reaction kinetics were essentially unchanged over the first 10 h, the reaction became much faster afterward and reached 77% after 19 h (vs. 64% after 25 h at 70°C, Figure S10). The molar masses of the recovered PMA samples were greater than the expected ones, and their dispersities were much broader ($Đ$ = 1.34–2.05) than those of the PMA samples prepared at 70°C (Tables S2, Figure S11). Altogether, these results indicate that operating at higher temperatures is not a good option for improving the initiator efficiency factor and the polymerization control.

Mechanistic considerations bring us to the question of the primary radical structure. To confirm whether AcO$^{\bullet}$ is the primary radical initiating the polymerization, its presence at the α-chain-end position must be demonstrated. To this end, a PMA sample of low molar mass, obtained by 1-propanethiol quenching after a short polymerization period (MA/**1** = 100, 3 h, 15% conv., M_n = 6100 g/mol, $Đ$ = 1.25, see Experimental Section for details), was isolated and analyzed by NMR and MALDI-ToF MS. The treatment with thiol of the polymer chain synthesized by OMRP is able to replace the cobalt complex with an H atom at the ω chain-end (Figure S12) [64]. The MALDI-ToF mass spectrum of the isolated PMA sample revealed the presence of three isotopic envelopes, each one exhibiting the expected separation of 86.1 g/mol (corresponding to one MA unit) between subsequent peaks (Figures S13–S16). The first population, corresponding to the most abundant envelope, has m/z values consistent with the presence of a hydrogen atom at both α and ω chain-ends and sodium as a cationizing agent from the matrix (Figure S14). The second population has a similar formula; however, it presents a potassium ion as a cationizing agent instead of sodium (Figure S15). The isotopic distribution of the third population is consistent with an H atom at the ω chain-end and a Me group at the α chain-end (Figure S16), in agreement with an initiation process involving a decarboxylation step (see Figure 8, blue pathway), and with the NMR analyses (see below). For all populations, the presence of an H atom at one chain end is expected to result from the 1-propanethiol quenching process. The presence of a H atom at the second chain-end in the major populations suggests that, at the early stage of the OMRP process, a β-H transfer from the unimer radical species (AcO-$CH_2C^{\bullet}$(H)CO_2Me) to the [(Salen*)Co^{II}] complex occurs, leading to the (AcO-CH = $CHCO_2$Me) molecule and the corresponding [(Salen*)Co^{III}—H] complex, which then initiates the OMRP of MA (see Figure 8, green pathway). The pseudo-living character of the MA polymerization (see above) excludes the occurrence of extensive CCT, furthermore supported by the absence of polymer chains with unsaturated chain-end (see Figures S17–S20), therefore we ruled out the occurrence of β-H transfer from the PMA$^{\bullet}$ propagating species, even originating from the Me$^{\bullet}$ initiation or from Co—H initiation (see Figure 8, orange pathway). PMA chains capped by an H atom at the ω chain-end (PrSH quenching) and an AcO group at the α chain-end, resulting from the AcO$^{\bullet}$ initiation, are another population that could be anticipated to be observed by MALDI-ToF analysis (see Figure 8, purple pathway), but no signal corresponding to such structure was observed. NMR data obtained for the same sample support the latter suggestions. Indeed, the ^{1}H, COSY, and HSQC NMR experiments (see Figures S17–S20) revealed the presence of a signal at δ = 1.15 ppm, attributed to a Me group at the α chain-end, that originates from the OAc initiating group after decarboxylation. On the other hand, no signal attributable to an OAc α chain-end could be observed. Indeed, such a signal should appear in a more downfield-shifted region in the ^{1}H NMR spectrum compared to a Me group (e.g., δ = 2.05 ppm for CH_3—C(O)OEt in $CDCl_3$), where intense signals of the PMA CH_2

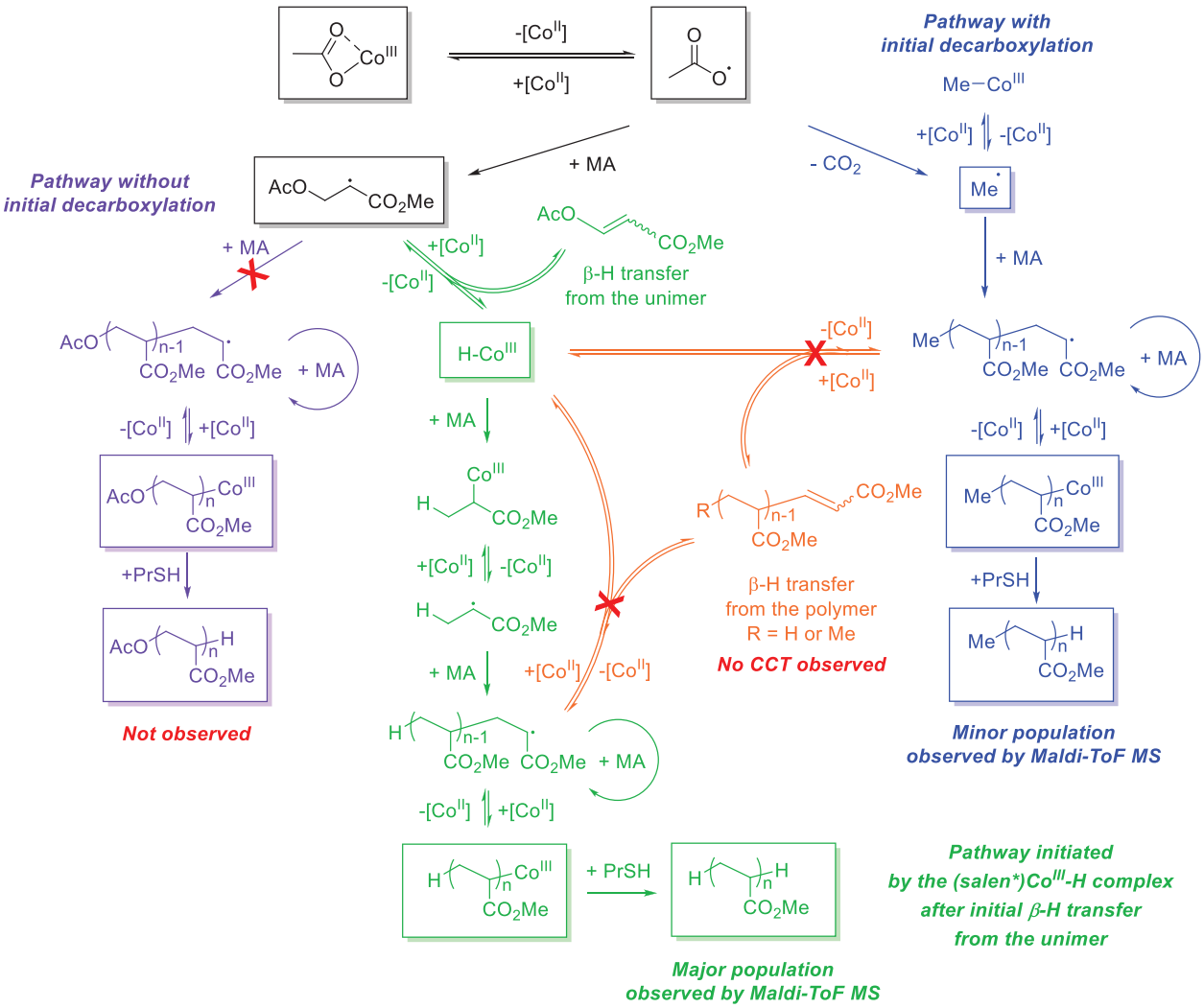

FIGURE 8 | Proposed mechanisms leading to different populations observed by MALDI-ToF mass spectrometry.

groups are present. As a confirmation, no signal corresponding to the methyl of the terminal acetate function was observed in the HSQC spectrum (Figure S20) at the expected chemical shifts of 2 ppm for ^{1}H and 21 ppm for ^{13}C.

2.5 | Chain-Extension Reaction

A PMA macroinitiator of low molar mass (M_n = 5100 g/mol, $Đ$ = 1.18) was first prepared as described in Figure 9 (left) and isolated (see Experimental Section) under strictly controlled conditions to avoid loss of the cobalt complex from the ω chain end. The latter was then reactivated in bulk butyl acrylate (BA) at 70°C (BA/Macroinitiator = 750) for 18 h, to yield the corresponding PMA-*b*-PBA block copolymer (Figure 9, left). The success of the chain-extension experiment could be established by GPC and ^{1}H DOSY NMR analyses. While the (Salen*)Co-PMA macroinitiator exhibited a monomodal distribution with M_n = 5 100 g/mol and $Đ$ = 1.18 (Figure 9, right, blue signal), the GPC signal clearly shifted to a higher molar mass (M_n = 29 200 g/mol, $Đ$ = 1.48, Figure 9, right, orange signal) and remained monomodal after the chain-extension, although with an evident tailing at low molar masses. Moreover, the ^{1}H DOSY NMR spectrum (Figure S21) of the recovered polymer shows the O—CH_3 and O—CH_2 characteristic signals of the PMA and PBA blocks, respectively, on the same diffusion line. Altogether, these results confirm the occurrence of chain extension, rather than BA homopolymerization.

This experiment highlights the living character of acrylate polymerization using the system reported here by evidencing the presence of the cobalt complex at the polymer chain-end, thereby enabling macromolecular engineering. Nevertheless, as previously demonstrated [64], the addition of nitroxides or alkanethiols to polymers prepared by cobalt-mediated radical polymerization allows for the almost quantitative removal of cobalt from the polymer.

3 | Conclusions

We have shown that the easily accessible and air-stable [(Salen*)Co(OAc)] complex **1** acts as an unimolecular initiator and moderator for radical polymerization processes. Catalyzed chain-transfer (CCT) was identified as the predominant mechanism for the radical polymerization of MMA, whereas a well-controlled chain growth takes place in the radical polymerization

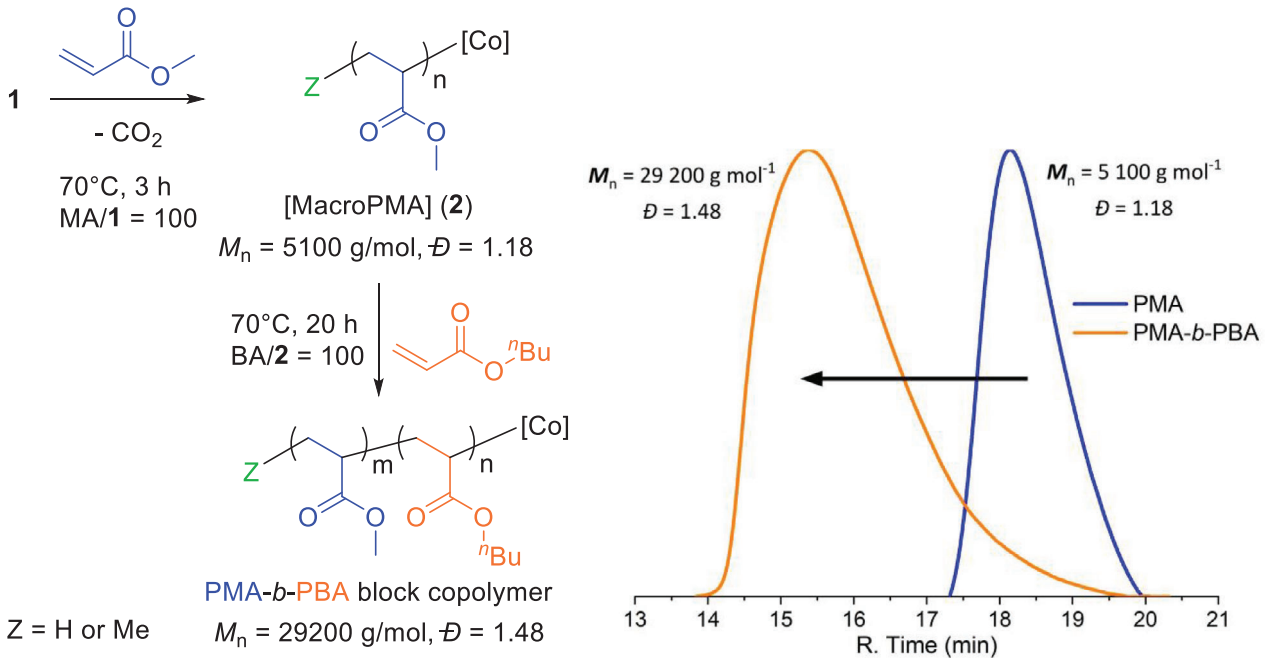

FIGURE 9 | Synthesis of a PMA macroinitiator and of a PMA-*b*-PBA block copolymer via OMRP initiated and mediated by complex **1** (left) and corresponding GPC traces (right). The M_n and $Đ$ values were determined by GPC using PMMA standards.

of MA in bulk at 70°C. However, complex **1** exhibited a moderate initiator efficiency. MALDI-ToF MS and multinuclear NMR analyses of the PMA produced with complex **1** as initiator revealed two mechanisms of initiation. One mechanism involves the preliminary Co^{III}—OAc bond homolysis, followed by decarboxylation of the $^{\bullet}$OAc radical species, and the resulting Me$^{\bullet}$ radical initiates the OMRP process, leading to α-Me PMA chains. Another mechanism involves the addition of the $^{\bullet}$OAc radical, prior to decarboxylation, to one MA molecule, and the resulting unimer undergoes a β-H elimination process, leading to a dead small unsaturated molecule and a Co—H initiating species that generates α-H-terminated PMA chains. The livingness of the OMRP of acrylates mediated by complex **1** could be further established by a chain-extension experiment, leading to the formation of a well-defined PMA-*b*-PBA block copolymer. These findings contribute to the development of novel (bench-stable) initiators for OMRP, supporting innovative strategies for polymer design.

4 | Experimental Section

4.1 | General Considerations

4.1.1 | Materials

TEMPO (1-oxy-2,2,6,6-tetramethylpiperidine, Apollo Scientific), 1-propanethiol (99%, Sigma-Aldrich), $Co(OAc)_2$ (anhydrous cobalt(II) diacetate, 98%, Alfa Aesar), 3,5-di-*tert*-butyl-2-hydroxybenzaldehyde (Apollo Scientific), (1R,2R)-(-)-1,2-diaminocyclohexane (Apollo Scientific), 1,3,5-trioxane (≥99%, Sigma-Aldrich) and $CDCl_3$ (99.8%D, Euriso-top) were used as received. Vinyl acetate (VAc), methyl meythacrylate (MMA), and methyl acrylate (MA) were purchased from Acros Organics (≥99%), dried over CaH_2, distilled under static vacuum, and stored under argon. Laboratory Reagent grade (99.5%) diethyl ether, *n*-pentane, dichloromethane, toluene, and methanol were purchased from Sigma-Aldrich and used as received. Complex **1** was synthesized according to a previously reported procedure, and its purity was confirmed by ^{1}H and $^{13}C\{^1H\}$ NMR and by elemental analysis [49].

4.1.2 | Characterizations

All NMR spectra were recorded on a Bruker Avance III 300 or 400 MHz spectrometer at, unless otherwise specified, ambient temperature. The ^{1}H and ^{13}C chemical shifts (δ) were determined using the residual ^{1}H solvent peak as the internal standard and reported in ppm versus $SiMe_4$. The $M_{n,exp,}$ and $Đ$ of the polymers were determined by GPC using a Shimadzu system equipped with a Shimadzu RID-20A refractive index detector with two PSS SDV analytical columns (1000 and 100 000 Å, 5 µm, 8 × 300 mm). THF was used as the eluent at a flow rate of 1 mL/min at 35°C. Linear PMMA standards were used for calibration. MALDI-ToF mass spectra were recorded by the technical staff of the mass spectrometry platform of the Toulouse Institute of Chemistry on a Q-Tof Premier (Waters) instrument using nitrogen as a drying agent and nebulizing gas and MeCN as solvent. The acquisition software was Masslynx (Waters), and the spectra were processed using Masslynx and Polymerix 3.0 (Sierra Analytics).

4.2 | Typical Procedure for a Polymerization Initiated by Complex 1

In a glovebox, complex **1** (50 mg, 0.075 mmol) was placed into a flame-dried Schlenk tube equipped with a magnetic stirring bar. The desired dry and degassed monomer (100 or 200 equiv. vs. **1**) was then added by syringe, and the tube was sealed with a rubber

septum. The resulting brown mixture was stirred and heated at the chosen reaction temperature in the dark. Aliquots were withdrawn from the reaction mixture at the desired times. Each of these aliquots was separated into two fractions. One fraction was used to determine the conversion by gravimetry (evaporation of the residual monomer under vacuum until constant weight). The other fraction was used to isolate a polymer sample after precipitation by the addition of pentane, washing, and drying under vacuum. The dried polymers were then dissolved in THF (at concentrations between 3 and 5 mg/mL) for the GPC analyses.

4.3 | TEMPO Quenching Reactions

For a specific polymerization reaction and at the desired reaction time, an aliquot was withdrawn from the reaction mixture, and the monomer conversion was determined by gravimetry. At the same reaction time, a solution of TEMPO (100 mg) in dry toluene (1 mL) under argon was injected into the polymerization reaction mixture. The evolution of the monomer conversion was then followed over the desired duration by gravimetry from aliquots withdrawn from the reaction mixture at several reaction times.

4.4 | Synthesis of a Short PMA Sample by 1-Propanethiol Quenching for MALDI-ToF Analysis

Complex **1** (132 mg, 0.20 mmol) was placed in a flame-dried Schlenk tube under argon, equipped with a magnetic stirring bar, and three vacuum argon cycles were applied. Dry and degassed MA (1.8 mL, 1.72 g, 20 mmol, MA/**1** ratio = 100) was added by syringe. The reaction mixture was then plunged into an oil bath at 70°C. After 3 h, aliquots were withdrawn and quenched with TEMPO for the NMR and GPC analyses. To the residual reaction mixture, 1-propanethiol (45.7 mg, 0.60 mmol) was added to quench the polymerization, and the resulting mixture was further stirred for 1 h at 70°C before removal of the residual monomer under vacuum. The residue was dissolved in acetone and filtered. Heptane was added dropwise into the filtrate and the precipitated polymer was collected and dried at 60°C under vacuum. The PMA sample was analyzed by ^{1}H, ^{13}C{^{1}H}, COSY, and HSQC NMR, and by MALDI-ToF MS (see ESI).

4.5 | Synthesis of a PMA-*b*-PBA Bock Copolymer via OMRP Using Complex 1

4.5.1 | Synthesis of the PMA Macroinitiator

In a glovebox, solid complex **1** (100 mg, 0.15 mmol) was placed in a flame-dried Schlenk tube equipped with a magnetic stirring bar. Dry and degassed MA (1.35 mL, 1.30 g, 15 mmol, MA/**1** ratio = 100) was then added by syringe and the tube was sealed with a rubber septum. The resulting brown mixture was stirred and heated at 70°C for 3 h in the dark. An aliquot was withdrawn from the reaction mixture to determine the monomer conversion and characterize the PMA macroinitiator by GPC. The remaining mixture was dried under vacuum and the residue was washed twice with pentane to remove any trace of unreacted MA. Conversion: 13%. M_n = 5100 g/mol, $Đ$ = 1.18.

4.5.2 | Chain-Extension Experiment

Dry and degassed BA (2.16 mL, 1.94 g, 15 mmol, BA/Co ratio = 750) was added by syringe to the previously synthesized PMA macroinitiator (100 mg, 0.02 mmol based on MW = 5100 g/mol) and the tube was sealed with a rubber septum. The resulting mixture was stirred and heated at 70°C for 24 h in the dark. An aliquot was withdrawn from the reaction mixture to determine the monomer conversion. The remaining mixture was dried under vacuum and the residue was washed twice with pentane to remove any trace of unreacted BA. The isolated brown solid was analyzed by GPC, ^{1}H NMR, and ^{1}H DOSY NMR. Conversion: 66%. M_n = 29 200 g/mol, $Đ$ = 1.48.

4.5.3 | Computational Details

The computational work was carried out using the Gaussian09 suite of programs [65]. Gas-phase geometry optimizations were performed without any symmetry constraint using the B3PW91* functional, which is a reparametrized version of B3PW91 with the same parameters previously optimized for B3LYP [66], and the 6-311G(d,p) basis functions for all light atoms (H, C, N, and O), whereas the Co atom was treated with the SDD basis set augmented by an f polarization function (α = 2.780) [67]. The unrestricted formulation was used for open-shell molecules, which typically yielded only minor spin contamination for all mononuclear systems ($<S^2>$ at convergence was very close to the expected values, namely 0.75 for doublet states). All final geometries were characterized as local minima by verifying that all second derivatives of the energy were positive. Corrections for dispersion were carried during the B3PW91* geometry optimizations using Grimme's D3 empirical method (BPW91*-D3), using SR6 and S8 parameters identical to those optimized for B3PW91 [68]. Thermochemical corrections were obtained on the fixed optimized geometries at 298.15 K on the basis of frequency calculations, using the standard approximations (ideal gas, rigid rotor, and harmonic oscillator). A correction of 1.95 kcal/mol was applied to bring the *G*-values from the gas phase (1 atm) to the solution (1 mol/L) standard state [69]. The Cartesian coordinates, electronic energies, and 1M-corrected Gibbs energies of all geometry-optimized molecules are available in Table S4.

Author Contributions

Maxime Michelas: investigation, formal analysis, writing – original draft. **Sofia McGee-Renedo:** investigation, formal analysis, writing – reports. **Jirong Wang:** investigation, formal analysis, writing – reports. **Rinaldo Poli:** investigation (DFT), formal analysis, writing – review and editing. **Antoine Debuigne:** conceptualization, supervision, writing – review and editing. **Christophe Fliedel:** conceptualization, funding acquisition, supervision, writing – review and editing. The manuscript was written through the contributions of all authors. All authors have given approval to the final version of the manuscript.

Acknowledgements

The authors gratefully acknowledge funding by the ANR (Agence Nationale de la Recherche) through the POLYSWITCH project (grant ANR-19-CE07-0031-01) and by the CNRS (Centre National de la Recherche Scientifique). R.P. is also grateful to the CALMIP mesocenter of

the University of Toulouse for the allocation of computational resources. A.D. is FNRS Senior Research Associate and is grateful to the F.R.S.-FNRS. The authors thank Zhuoqun Wang for the fruitful discussions and for her help in setting up some experiments and Jadhe Salin for performing some polymerization reactions and GPC analyses.

Conflicts of Interest

The authors declare no conflicts of interest.

Data Availability Statement

The data that support the findings of this study are openly available in https://hal.science/ at 10.1002/macp.202500204.

References

1. N. Corrigan, K. Jung, G. Moad, C. J. Hawker, K. Matyjaszewski, and C. Boyer "Reversible-deactivation Radical Polymerization (Controlled/living radical polymerization): From Discovery to Materials Design and Applications," *Progress in Polymer Science* 111 (2020): 101311.

2. W. A. Braunecker, and K. Matyjaszewski "Controlled/Living Radical Polymerization: Features, Developments, and Perspectives," *Progress in Polymer Science* 32 (2007): 93–146.

3. E. J. Cornel, J. Jiang, S. Chen, and J. Du "Principles and Characteristics of Polymerization-Induced Self-Assembly With Various Polymerization Techniques," *CCS Chemistry* 3, no. 4 (2020): 2104–2125.

4. T. A. Von Werne, D. S. Germack, E. C. Hagberg, V. V. Sheares, C J. Hawker, and K R. Carter "A Versatile Method for Tuning the Chemistry and Size of Nanoscopic Features by Living Free Radical Polymerization," *Journal of the American Chemical Society* 125, no. 13 (2003): 3831–3838.

5. J. Pyun, S. Jia, T. Kowalewski, G. D. Patterson, and K. Matyjaszewski "Synthesis and Characterization of Organic/Inorganic Hybrid Nanoparticles: Kinetics of Surface-Initiated Atom Transfer Radical Polymerization and Morphology of Hybrid Nanoparticle Ultrathin Films," *Macromolecules* 36, no. 14 (2003): 5094–5104.

6. K. Matyjaszewski "Advanced Materials by Atom Transfer Radical Polymerization," *Advanced Materials* 30, no. 23 (2018): 1706441.

7. C. Boyer, N. A. Corrigan, and K. Jung et al., "Copper-Mediated Living Radical Polymerization (Atom Transfer Radical Polymerization and Copper(0) Mediated Polymerization): From Fundamentals to Bioapplications," *Chemistry A European Journal* 116, no. 4 (2016): 1803–1949.

8. K. Matyjaszewski, and N. V. Tsarevsky "Nanostructured Functional Materials Prepared by Atom Transfer Radical Polymerization," *Nature Chemistry* 1, no. 4 (2009): 276–288.

9. S. Perrier "50th Anniversary Perspective : RAFT Polymerization—A User Guide," *Macromolecules* 50, no. 19 (2017): 7433–7447.

10. T. G. Ribelli, F. Lorandi, M. Fantin, and K. Matyjaszewski "Atom Transfer Radical Polymerization: Billion Times More Active Catalysts and New Initiation Systems," *Macromolecular Rapid Communications* 40, no. 1 (2019): 1800616.

11. K. Matyjaszewski "Atom Transfer Radical Polymerization (ATRP): Current Status and Future Perspectives," *Macromolecules* 45, no. 10 (2012): 4015–4039.

12. K. Matyjaszewski, and J. Xia "Atom Transfer Radical Polymerization," *Chemical Review* 101 (2001): 2921–2990.

13. L. E. N. Allan, M. R. Perry, and M. P. Shaver "Organometallic Mediated Radical Polymerization," *Progress in Polymer Science* 37, no. 1 (2012): 127–156.

14. M. Hurtgen, C. Detrembleur, C. Jerome, and A. Debuigne "Insight Into Organometallic-Mediated Radical Polymerization," *Polymer Reviews* 51, no. 2 (2011): 188–213.

15. R. Poli "Radical Coordination Chemistry and Its Relevance to Metal-Mediated Radical Polymerization," *European Journal of Inorganic Chemistry*, no. 10 (2011): 1513–1530.

16. R. Poli "Relationship Between One-Electron Transition-Metal Reactivity and Radical Polymerization Processes," *Angewandte Chemie International Edition* 45, no. 31 (2006): 5058–5070.

17. L. Thevenin, C. Fliedel, K. Matyjaszewski, and R. Poli "Impact of Catalyzed Radical Termination (CRT) and Reductive Radical Termination (RRT) in Metal-Mediated Radical Polymerization Processes," *European Journal of Inorganic Chemistry*, no. 42 (2019): 4489–4499.

18. R. Poli "New Phenomena in Organometallic-Mediated Radical Polymerization (OMRP) and Perspectives for Control of Less Active Monomers," *Chemistry A European Journal* 21, no. 19 (2015): 6988–7001.

19. A N. Morin, C. Detrembleur, C. Jérôme, P. De Tullio, R. Poli, and A. Debuigne "Effect of Head-to-Head Addition in Vinyl Acetate Controlled Radical Polymerization: Why Is Co(acac) 2 -Mediated Polymerization so Much Better?," *Macromolecules* 46, no. 11 (2013): 4303–4312.

20. A. Debuigne, J.-R. Caille, and R. Jérôme "Highly Efficient Cobalt-Mediated Radical Polymerization of Vinyl Acetate," *Angewandte Chemie International Edition* 44, no. 7 (2005): 1101–1104.

21. A. Debuigne, A. N. Morin, and A. Kermagoret et al., "Key Role of Intramolecular Metal Chelation and Hydrogen Bonding in the Cobalt-Mediated Radical Polymerization of N -Vinyl Amides," *Chemistry A European Journal* 18, no. 40 (2012): 12834–12844.

22. A. Debuigne, M. Schoumacher, and N. Willet et al., "New Functional Poly(N-vinylpyrrolidone) Based (co)Polymers via Photoinitiated Cobalt-mediated Radical Polymerization," *Chemical Communications* 47, no. 47 (2011): 12703.

23. S. Banerjee, V. Ladmiral, A. Debuigne, C. Detrembleur, R. Poli, and B. Améduri "Organometallic-Mediated Radical Polymerization of Vinylidene Fluoride," *Angewandte Chemie International Edition* 57, no. 11 (2018): 2934–2937.

24. C. Fliedel, and R. Poli "Homolytically weak metal-carbon bonds make robust controlled radical polymerizations systems for "less-activated monomers"," *Journal of Organometallic Chemistry* 880 (2019): 241–252.

25. A. Debuigne, C. Jérôme, and C. Detrembleur "Organometallic-mediated Radical Polymerization of 'Less Activated Monomers': Fundamentals, Challenges and Opportunities," *Polymer* 115 (2017): 285–307.

26. J. Demarteau, A. Debuigne, and C. Detrembleur "Organocobalt Complexes as Sources of Carbon-Centered Radicals for Organic and Polymer Chemistries," *Chemical Review* 119, no. 12 (2019): 6906–6955.

27. C.-H. Peng, T.-Y. Yang, Y. Zhao, and X. Fu "Reversible Deactivation Radical Polymerization Mediated by Cobalt Complexes: Recent Progress and Perspectives," *Organic and Biomolecular Chemistry* 12, no. 43 (2014): 8580–8587.

28. A. Debuigne, R. Poli, C. Jérôme, R. Jérôme, and C. Detrembleur "Overview of Cobalt-mediated Radical Polymerization: Roots, state of the Art and Future Prospects," *Progress in Polymer Science* 34, no. 3 (2009): 211–239.

29. K. M. Smith, W. S Mcneil, and A. S. Abd-El-Aziz "Organometallic-Mediated Radical Polymerization: Developing Well-Defined Complexes for Reversible Transition Metal-Alkyl Bond Homolysis," *Macromolecular Chemistry and Physics* 211, no. 1 (2010): 10–16.

30. R. Poli "Organometallic Mediated Radical Polymerization," in *Polymer Science: A Comprehensive Reference*, eds. K. Matyjaszewski, M. Moller, (Elsevier BV, 2012), 351–375.

31. R. Poli, L. E. N. Allan, and M. P. Shaver "Iron-mediated Reversible Deactivation Controlled Radical Polymerization," *Progress in Polymer Science* 39, no. 10 (2014): 1827–1845.

32. C. Fliedel, S. Dagorne, and E. Le Roux "9.14 - Metal Complexes as Catalysts/Moderators for Polymerization Reactions," in *Comprehensive Coordination Chemistry III*, eds. E. C. Constable, G. Parkin, L. Que (Elsevier, 2021), 410–464.

33. M. Michelas, and C. Fliedel "Poli, R. 1.03 - Reversible Homolysis of Metal-Carbon Bonds," in *Comprehensive Organometallic Chemistry IV*, eds. G. Parkin, K. Meyer, D. O'hare (Elsevier, 2022), 31–85.

34. C.-M. Liao, C.-C. Hsu, F.-S Wang, B. B. Wayland, and C.-H. Peng "Living Radical Polymerization of Vinyl Acetate and Methyl Acrylate Mediated by Co(Salen*) Complexes," *Polymer Chemistry* 4, no. 10 (2013): 3098.

35. C.-H. Peng, S. Li, and B. B. Wayland "Formation and Interconversion of Organo-cobalt Complexes in Reactions of Cobalt(II) Porphyrins With Cyanoalkyl Radicals and Vinyl Olefins," *Inorganic Chemistry* 48, no. 11 (2009): 5039–5046.

36. A. Kermagoret, A. Debuigne, C. Jérôme, and C. Detrembleur "Precision Design of Ethylene- and Polar-monomer-based Copolymers by Organometallic-mediated Radical Polymerization," *Nature Chemistry* 6, no. 3 (2014): 179–187.

37. K. Santhosh, Y. Gnanou, Y. Champouret, J. C. Daran, and R. Poli, "Radical Polymerization of Vinyl Acetate With Bis(tetramethylheptadionato)Cobalt(II): Coexistence of Three Different Mechanisms," *Chemistry A European Journal* 15, no. 19 (2009): 4874–4885.

38. W. Benchaphanthawee, and C.-H. Peng "Organo-Cobalt Complexes in Reversible-Deactivation Radical Polymerization," *The Chemical Record* 21, no. 12 (2021), 3628–3647.

39. R. Bryaskova, C. Detrembleur, A. Debuigne, and R. Jérôme "Cobalt-Mediated Radical Polymerization (CMRP) of Vinyl Acetate Initiated by Redox Systems: Toward the Scale-Up of CMRP," *Macromolecules* 39, no. 24 (2006): 8263–8268.

40. J. Demarteau, A. Kermagoret, and I. German et al., "Halomethylcobalt(bis-acetylacetonate) for the Controlled Synthesis of Functional Polymers," *Chemical Communications* 51, no. 76 (2015): 14334–14337.

41. M. Michelas, J.-C. Daran, A. Sournia-Saquet, C. Fliedel, and R. Poli "A mononuclear cobalt(iii) carboxylate complex With a fully O-based coordination sphere: Co III –O bond homolysis and controlled radical polymerization From [Co(acac) 2 (O 2 CPh)]," *Dalton Transactions* 52, no. 20 (2023): 6791–6798.

42. L. Chiang, L. E. N. Allan, J. Alcantara, M. C. P. Wang, T. Storr, and M. P. Shaver "Tuning Ligand Electronics and Peripheral Substitution on Cobalt Salen Complexes: Structure and Polymerisation Activity," *Dalton Transactions* 43, no. 11 (2014): 4295–4304.

43. Y. Zhao, Y. Wang, and X. Zhou et al., "Oxygen-Triggered Switchable Polymerization for the One-Pot Synthesis of CO 2 -Based Block Copolymers From Monomer Mixtures," *Angewandte Chemie International Edition* 58, no. 40 (2019): 14311–14318.

44. Y. Wang, Y. Zhao, and S. Zhu et al., "Switchable Polymerization Triggered by Fast and Quantitative Insertion of Carbon Monoxide Into Cobalt–Oxygen Bonds," *Angewandte Chemie International Edition* 59, no. 15 (2020): 5988–5994.

45. Y. Zhao, M. Yu, and S. Zhang et al., "A well-defined, versatile photoinitiator (salen)Co–CO 2 CH 3 for visible light-initiated living/controlled radical polymerization," *Chemical Science* 6, no. 5 (2015): 2979–2988.

46. S. E. Schaus, B. D. Brandes, and J. F. Larrow et al., "Highly Selective Hydrolytic Kinetic Resolution of Terminal Epoxides Catalyzed by Chiral (salen)CoIII Complexes. Practical Synthesis of Enantioenriched Terminal Epoxides and 1,2-Diols," *Journal of the American Chemical Society* 124, no. 7 (2002): 1307–1315.

47. M. Tokunaga, J. F. Larrow, F. Kakiuchi, and E. N. Jacobsen "Asymmetric Catalysis With Water: Efficient Kinetic Resolution of Terminal Epoxides by Means of Catalytic Hydrolysis," *Science* 277, no. 5328 (1997): 936–938.

48. E. N. Jacobsen, F. Kakiuchi, R. G. Konsler, J. F. Larrow, and M. Tokunaga "Enantioselective Catalytic Ring Opening of Epoxides With Carboxylic Acids," *Tetrahedron Letters* 38, no. 5 (1997): 773–776.

49. L. P. C. Nielsen, C. P. Stevenson, D. G. Blackmond, and E. N. Jacobsen "Mechanistic Investigation Leads to a Synthetic Improvement in the Hydrolytic Kinetic Resolution of Terminal Epoxides," *Journal of the American Chemical Society* 126, no. 5 (2004): 1360–1362.

50. X.-B. Lu, and Y. Wang "Highly Active, Binary Catalyst Systems for the Alternating Copolymerization of CO2 and Epoxides Under Mild Conditions," *Angewandte Chemie International Edition* 43, no. 27 (2004): 3574–3577.

51. D. J. Darensbourg "Making Plastics From Carbon Dioxide: Salen Metal Complexes as Catalysts for the Production of Polycarbonates From Epoxides and CO2," *Chemical Review* 107, no. 6 (2007): 2388–2410.

52. Z. Qin, C. M. Thomas, S. Lee, and G. W. Coates "Cobalt-Based Complexes for the Copolymerization of Propylene Oxide and CO 2 : Active and Selective Catalysts for Polycarbonate Synthesis," *Angewandte Chemie International Edition* 42, no. 44 (2003): 5484–5487.

53. J. F. Larrow, E. N. Jacobsen, Y. Gao, Y. Hong, X. Nie, and C. M. Zepp "A Practical Method for the Large-Scale Preparation of [N,N'-Bis(3,5-di-tertbutylsalicylidene)-1,2-cyclohexanediaminato(2-)]Manganese(III) Chloride, a Highly Enantioselective Epoxidation Catalyst," *Journal of Organic Chemistry* 59, no. 7 (1994): 1939–1942.

54. L. P. C. Nielsen, C. P. Stevenson, D. G. Blackmond, and E. N. Jacobsen "Mechanistic Investigation Leads to a Synthetic Improvement in the Hydrolytic Kinetic Resolution of Terminal Epoxides," *Journal of the American Chemical Society* 126 (2004): 1360–1362.

55. R. Thiagarajan, V. Kalpagam, and U. S. Nandi, "Mixed Ligand Complexes in Vinyl Polymerization. I. [N,N'-ethylenebis(salicylideneiminato)](acetylacetonato)cobalt(III) as an Initiator," *Journal of Polymer Science, Part A: Polymer Chemistry* 20, no. 3 (1982): 675–681.

56. M. Michelas, Y. K. Redjel, J.-C. Daran, M. Benslimane, R. Poli, and C. Fliedel "Cobalt(II) and Cobalt(III) Complexes of Tripodal Tetradentate Diamino-bis(phenolate) Ligands: Synthesis, Characterization, Crystal Structures and Evaluation in Radical Polymerization Processes," *Inorganica Chimica Acta* 549 (2023): 121408.

57. Y. K. Redjel, L. Thevenin, J.-C. Daran, M. Benslimane, R. Poli, and C. Fliedel "Acetylacetonato Cobalt(III) and Iron(III) Complexes of Picolylamine- and Aminopropylamine-bis(phenolate) Ligands: Synthesis, Characterization and Crystal Structures," *Polyhedron* 158, (2019): 83–90.

58. A. Cyriac, J. Y. Jeon, and J. K. Varghese et al., "Unusual Coordination Mode of Tetradentate Schiff Base Cobalt(III) Complexes," *Dalton Transactions* 41, no. 5 (2012): 1444–1447.

59. A. Debuigne, Y. Champouret, R. Jérôme, R. Poli, and C. Detrembleur "Mechanistic Insights Into the Cobalt-Mediated Radical Polymerization (CMRP) of Vinyl Acetate With Cobalt(III) Adducts as Initiators," *Chemistry A European Journal* 14, no. 13 (2008): 4046–4059.

60. S. Maria, H. Kaneyoshi, K. Matyjaszewski, and R. Poli "Effect of Electron Donors on the Radical Polymerization of Vinyl Acetate Mediated by [Co(acac) 2]: Degenerative Transfer versus Reversible Homolytic Cleavage of an Organocobalt(III) Complex," *Chemistry A European Journal* 13, no. 9 (2007): 2480–2492.

61. E. V. Bellan, L. Thevenin, F. Gayet, C. Fliedel, and R. Poli "Catalyzed Chain Transfer in Vinyl Acetate Polymerization Mediated by 9-Oxyphenalenone Cobalt(II) Complexes," *Acs Macro Letters* 6, (2017): 959–962.

62. A. A. Gridnev, and S. D. Ittel "Catalytic Chain Transfer in Free-Radical Polymerizations," *Chemical Reviews* 101, (2001): 3611–3660.

63. J. P. A. Heuts, and N. M. B. Smeets "Catalytic Chain Transfer and Its Derived Macromonomers," *Polymer Chemistry* 2, no. 11 (2011): 2407.

64. A. Debuigne, J.-R. Caille, and R. Jérôme "Synthesis of End-functional Poly(vinyl acetate) by Cobalt-mediated Radical Polymerization," *Macromolecules* 38, no. 13 (2005): 5452–5458.

65. M. J. Frisch, G. W. Trucks, H. B. Schlegel, et al., *Gaussian 09, Revision D.01*, (Gaussian, Inc., 2009).

66. M. Reiher "Theoretical Study of the Fe(phen)2(NCS)2 Spin-Crossover Complex With Reparametrized Density Functionals," *Inorganic Chemistry* 41, no. 25 (2002): 6928–6935.

67. A. W. Ehlers, M. Böhme, and S. Dapprich et al., "A set of f-polarization functions for pseudo-potential basis sets of the transition metals Sc Cu, Y Ag and La Au," *Chemical Physics Letters* 208, no. 1 (1993): 111–114.

68. S. Grimme, J. Antony, S. Ehrlich, and H. Krieg "A Consistent and Accurate Ab Initio Parametrization of Density Functional Dispersion Correction (DFT-D) for the 94 Elements H-Pu," *Journal of Chemical Physics* 132, no. 15 (2010): 154104.

69. V. S. Bryantsev, M. S. Diallo, and W. A. Goddard Iii "Calculation of Solvation Free Energies of Charged Solutes Using Mixed Cluster/Continuum Models," *Journal of Physical Chemistry B* 112, no. 32 (2008): 9709–9719.

Supporting Information

Additional supporting information can be found online in the Supporting Information section.

Supporting File 1: macp70058-sup-0001-SuppMat.pdf.